*J. Fluid Mech.* (2009), *vol.* 618, *pp.* 349–359. © 2008 Cambridge University Press
doi:10.1017/S0022112008004400 Printed in the United Kingdom


# The effect of drainage on the capillary retention of $CO_2$ in a layered permeable rock

ADRIAN FARCAS AND ANDREW W. WOODS†
BP Institute, Cambridge, CB3 OEZ, UK

(Received 8 May 2008 and in revised form 22 September 2008)

Buoyant plumes of $CO_2$ spreading through water-saturated permeable rock, bounded by layers of lower permeability, tend to spread laterally. As they advance, they may gradually leak through fractures or discontinuities in the lower permeability boundary, leading to a gradual waning of the original plume and dispersal of $CO_2$ higher in the formation. With a finite release of $CO_2$, the trailing edge of the plume recedes with time, and capillary forces tend to trap a fraction of this $CO_2$ within the pore space. This also leads to a gradual waning of the plume with time and limits the mass of $CO_2$ which can leak through the boundary and rise higher into the formation. We explore the balance between these two effects and calculate some of the controls on the fraction of the $CO_2$ plume which becomes trapped within the original layer of rock.

## 1. Introduction

The continued emission of large volumes of anthropogenic $CO_2$ into the atmosphere, and the present trend of global warming, have stimulated considerable interest in the possible sequestration of $CO_2$ into deep subsurface aquifers or depleted oil and gas fields. A number of studies have been carried out to explore some of the dynamic controls on the dispersal of such $CO_2$ plumes within the subsurface, and there are a number of live $CO_2$ sequestration schemes in operation (Hesse, Tchelepi & Orr 2006; Bickle *et al.* 2007; Nordbotten & Celia 2006; Obi & Blunt 2006; Hesse *et al.* 2007). One of the most notable is the $CO_2$ injection facility at the Sleipner field in the North Sea, and there is also injection in the In Salah gas field in Algeria and the Weyburn field in Canada. With deep injection, $CO_2$ takes the form of a supercritical fluid, with density of the order 600–700 kg $m^{-3}$ and viscosity of the order $10^{-4}$ Pa s. $CO_2$ is highly buoyant in a water-saturated system and tends to spread laterally along the upper boundary of any high-permeability layer into which it is injected. A number of studies have developed quantitative descriptions for the rate of dispersal of $CO_2$ plumes in such a situation, developing scaling laws for the along-layer speed of the current in terms of the injection rate or the injected volume of fluid (Mitchell & Woods 2006; Nordbotten & Celia 2006; Bickle *et al.* 2007; Hesse *et al.* 2007). In these models, the $CO_2$–water interface is approximated as a sharp front, and as the currents become long and thin, the pressure is assumed to be hydrostatic in the cross-slope direction.

One of the challenges in modelling the dispersal of such $CO_2$ plumes is the inclusion of some of the complicating effects associated with the interactions between the $CO_2$, water and rock (Kharaka *et al.* 2006; Nordbotten & Celia 2006) and also the effects

† Email address for correspondence: andy@bpi.cam.ac.uk

of layering in the rocks. At the leading edge of the current, a fraction of the original water is displaced by the $CO_2$ plume, and the remainder is trapped in the gas zone by capillary forces. This water is soluble in the $CO_2$, and as it dissolves into the $CO_2$, a second front develops across which there is a transition from wet to dry $CO_2$, and the trapped water phase dissolves into the gas (Nordbotten & Celia 2006). At the rear of the $CO_2$ plume, some of the $CO_2$ remains trapped in the pore spaces as water displaces it (Barenblatt 1996; Hesse *et al.* 2006; Hesse, Orr & Tchelepi 2008). The fraction of the pore space containing this trapped $CO_2$ may change depending on the detailed pore structure and the interfacial tension; recent modelling suggests the rear of the plume may be approximated as a front, with the residual $CO_2$ taking values in the range 0–0.3, although more experimental tests of the modelling would be valuable (Hesse *et al.* 2006; Kharaka *et al.* 2006; Qi *et al.* 2007). The water in contact with this residual $CO_2$, in the wake of the mobile $CO_2$ plume, tends to become saturated in $CO_2$, and hence it becomes relatively dense compared to the original aquifer water; this may ultimately lead to convective mixing with the original water in the aquifer, in the wake of the $CO_2$ plume (cf. Qi *et al.* 2007; Riaz *et al.* 2007).

As a result of the capillary retention, the volume of the spreading plume of $CO_2$ gradually wanes with time, in a fashion which has some similarity to that of a spreading mound of water in an unsaturated rock (cf. Barenblatt, Entove & Ryzhik 1990; Barenblatt 1996) or a boiling current of water (Woods 1998). The capillary trapping of the $CO_2$ at the trailing edge of the plume forms an important mechanism of sequestering the $CO_2$ in the aquifer. In our analysis, we follow the approach of Hesse *et al.* (2006) and treat the capillary retention across the receding front of $CO_2$ as a parameter in order to explore how the macroscopic behaviour of the $CO_2$ plume changes with the amount of capillary retention.

Secondly, as in the Sleipner field, offshore Norway, the rock often contains laterally extensive, low-permeability horizons, which constrain the plume to spread laterally except where there are localized faults, fractures or other discontinuities through which a fraction of the buoyant fluid can ascend and drain upwards through the formation (Pritchard, Woods & Hogg 2001; Pritchard 2007; Woods & Farcas 2009). In the case that the plume extends 1–10 km laterally, there may be very many such fractures, and the low permeability horizon may be characterized with a vertical permeability which scales as the average of the product of the vertical permeability and width of the faults per unit length along the boundary. The effect of the upward drainage of $CO_2$ through such a boundary is to deplete the plume and hence limit the capillary retention of $CO_2$ in the layer below the low-permeability horizon.

The purpose of this paper is to combine models of the capillary retention (Barenblatt 1996; Hesse *et al.* 2006) with models of drainage (Pritchard *et al.* 2001), to enable us to explore the balance between these competing processes; this is key, since it can determine the fraction of the initial $CO_2$ plume which is retained in the original layer by capillarity (cf. figure 1). We consider the dynamics of the plume in both a horizontal and an inclined layer, and we discuss the implications of our results for predicting and monitoring the dynamics of such $CO_2$ plumes in the subsurface. We focus on the case of injection from a horizontal well, so that the flow is approximately two-dimensional in the plane normal to the axis of the well; this corresponds to the injection regime at the In Salah gas field, in which the injection wells laterally extend more that 1 km within the repository rock. Analogous solutions could however be developed for the case of radial flow from the central well. In developing the model, we are primarily interested in the balance between the draining and the capillary

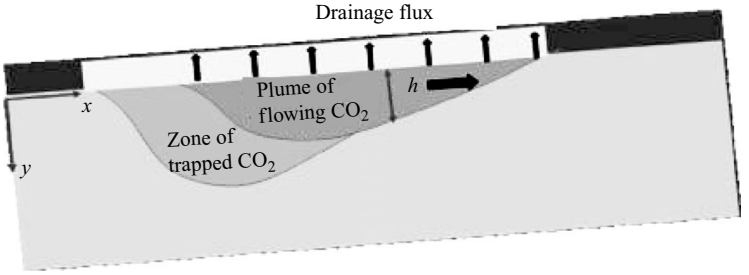


FIGURE 1. Illustration of the lateral migration of a plume of $CO_2$ along the upper low-permeability boundary of a permeable layer of rock. Fractures in this low-permeability layer can lead to an effective vertical permeability of the upper boundary, which enables the $CO_2$ to drain from the layer. The figure also illustrates the zone of trapped $CO_2$ which remains in the formation owing to capillary retention as water displaces the receding (trailing) edge of the plume.

retention, and so we simplify the model by neglecting the front between the dry and wet $CO_2$. There is only a small density change across this front, compared to the $CO_2$–water density contrast, so this front has little impact on the dynamics of the current and hence on the draining or capillary retention (Nordbotten & Celia 2006). Similarly, in order to calculate the capillary retention at the trailing edge of the gas plume as it advances upslope, we neglect any effects of the subsequent dissolution/convection of the trapped $CO_2$ in the wake of the $CO_2$ plume (cf. Hesse *et al.* 2006).

## 2. The model

We model the flow of a two-dimensional buoyant plume, released from a line source, with initial finite volume A per unit length and density $\rho_g$. We assume it spreads along a permeable layer of effective permeability $k$ and porosity $\phi$, initially saturated with the host fluid of density $\rho_w$. This corresponds, for example, to the post-injection phase of spreading of a $CO_2$ plume, in which the leading edge of the current advances into the water-saturated region of the rock, while there is a receding front of $CO_2$ as the trailing edge is displaced by water (figure 1). We assume that the plume advances updip through a permeable layer, adjacent to a thin, impermeable but fractured boundary, with effective permeability $k_b$ ($\ll k$) associated with the fractures and thickness $b$ (Pritchard *et al.* 2001; Pritchard 2007). As the plume spreads along the permeable inclined layer of rock, the flow becomes long and thin so that the cross-layer pressure gradient is approximately hydrostatic (Bear 1971; Huppert & Woods 1995):

$$p(x, y, t) = p_o - \rho_w g \cos\theta(x \tan\theta - h) - \rho_g g \cos\theta(h - y), \tag{1}$$

where $x$ is the along-layer coordinate, $y$ the cross layer coordinate, $h$ the depth of the plume normal to the boundary and $\theta$ the angle of slope to the horizontal. In our model, we follow Hesse *et al.* (2006) and Nordbotten & Celia (2006) who showed that both advancing and receding $CO_2$–water interfaces may be approximated as sharp fronts. Indeed, Nordbotten & Celia (2006) showed that solutions from the frontal model are analogous to the results of a full numerical simulation of the two-phase flow.

The drainage flux across the boundary, $Q$, is given by the balance between the excess hydrostatic pressure associated with the buoyant plume and the viscous dissipation across the fractures in the thin low-permeability layer (Pritchard *et al.* 2001; Pritchard

& Hogg 2002):

$$Q = \frac{k_b \Delta\rho g \cos\theta (h+b)}{\mu b}. \tag{2}$$

The along-slope pressure gradient in the $CO_2$ flow is given by Darcy's law, which involves a balance between the viscous dissipation of the flow, the pressure gradient and the along-slope component of gravity (cf. Bear 1971):

$$u = -\frac{k}{\mu}\left[\frac{\partial p}{\partial x} + \rho_g g \sin\theta\right]. \tag{3}$$

We assume the $CO_2$ flow is controlled by the effective permeability $k$. With capillary retention, in a region of the current in which the front ascends, $\partial h/\partial t > 0$; this leads to the dimensionless equation for the conservation of $CO_2$:

$$\frac{\partial \hat{h}}{\partial \hat{t}} = \frac{\partial}{\partial \hat{x}}\left(\hat{h}\frac{\partial \hat{h}}{\partial \hat{x}} - \hat{h}\tan\theta\right) - \Gamma(\hat{h}+\varepsilon). \tag{4}$$

In the above equation the $\hat{}$ notation denotes dimensionless variables; $\Gamma = k_b A^{1/2}/kb$; time is scaled relative to the time scale for flow along the layer,

$$\tau = \frac{A^{1/2}\phi\mu}{\Delta\rho g k \cos\theta}; \tag{5}$$

the space coordinates $h$ and $x$ are scaled relative to $A^{1/2}$, where $A$ is the initial area of the current; and $\varepsilon = b/A^{1/2}$. Also, in regions of the current in which the $CO_2$ plume recedes, $\frac{\partial h}{\partial t} < 0$, the governing equation for the depth has the form (cf. Barenblatt 1996; Hesse *et al.* 2006)

$$\beta\frac{\partial \hat{h}}{\partial \hat{t}} = \frac{\partial}{\partial \hat{x}}\left(\hat{h}\frac{\partial \hat{h}}{\partial \hat{x}} - \hat{h}\tan\theta\right) - \Gamma(\hat{h}+\varepsilon), \tag{6}$$

where $\beta$ denotes the fraction of the pore space flooded by the invading water front, and hence $1-\beta$ is the fraction of the pore space in which $CO_2$ is retained by capillarity. The locus of the receding front is given by the evolution with time of the point at which $\partial h/\partial t = 0$. The limit in which there is no capillary retention, $\beta = 1$, and the low permeability layer is very thin, $\varepsilon \sim 0$, admits a solution for the dispersal of a finite mass of the buoyant fluid as it drains through the low permeability layer (cf. Woods & Farcas 2008), given by

$$\hat{h} = \frac{6^{1/3}}{4}\exp(-\Gamma\hat{t})\tau^{-1/3}\left[1 - \frac{4(\hat{x}-\hat{t}\tan\theta)^2}{6^{4/3}\tau^{2/3}}\right] \text{ with } \tau = \frac{(1-\exp(-\Gamma\hat{t}))}{\Gamma}. \tag{7}$$

However, in general, with $\beta < 1$ and $1 \gg \varepsilon > 0$, the shape of the current is more complex. We now explore this competition between capillary retention and draining in the case of both horizontal and inclined boundaries. Using a generalization of the implicit Crank–Nicolson method for nonlinear diffusion (Press *et al.* 1992), (4) and (6) were integrated numerically. The space step ranged from 0.001 to 0.05, and the time step ranged from $10^{-8}$ to $10^{-2}$; all the results presented are robust to changes in resolution.

## 3. Horizontal boundary

We first consider the case of a horizontal boundary, $\tan\theta = 0°$, in which the flow is symmetrical, and we explore how the run-out distance and the fraction of the flow

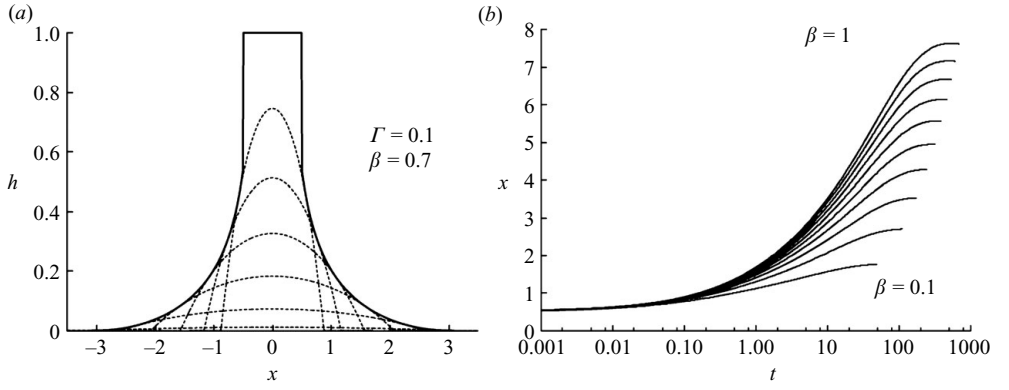


FIGURE 2. (*a*) Evolution of the thickness of a plume of $CO_2$ as a function of position as it spreads across a horizontal surface, draining through the boundary with the parameters $\Gamma = 0.1$, $\beta = 0.7$ and $\varepsilon = 0$. The profiles are taken at dimensionless time intervals 0, 0.1, 0.33, 1.0, 2.5, 7.5 and 20. (*b*) Variation with time of the position of the nose of a draining plume as it spreads beneath a horizontal boundary. In this figure, the drainage parameter $\Gamma$ has value 0.01, and $\varepsilon = 0$, while $\beta$ ranges from 0.1 to 1, in increments of 0.1, as shown. The value $\beta = 1$ corresponds to the case with no capillary retention in the pore spaces.

which is trapped by capillary retention varies with the draining rate ($\Gamma$), the fraction of the pore space flooded by water at the receding interface ($\beta$) and the dimensionless thickness of the seal layer ($\varepsilon$).

In figure 2(*a*) we show the evolution of the shape of the plume with time as it spreads laterally from the initial shape, $h = 1$ for $-0.5 < x < 0.5$ and $h = 0$ for $|x| > 0.5$; in this figure $\Gamma = 0.1$, $\beta = 0.7$ and $\varepsilon = 0$. Figure 2(*b*) illustrates how the position of the nose of the current increases with time in the case $\Gamma = 0.01$ and $\varepsilon = 0$ but with the range of $\beta = 0.1, 0.2, \ldots 1$. It is seen that at a given time, in the case of no capillary retention ($\beta = 1$) the plume has spread further from the source than the solutions with capillary retention ($\beta < 1$). Also, currents with less capillary retention have a greater final run-out distance and require considerably more time to reach this point. (Note in our numerical calculations the run-out distance is chosen as the point at which the current volume falls to $10^{-4}$ of the initial volume).

Figure 3(*a*) illustrates the variation of the final run-out distance as a function of $\Gamma$ and $\beta$ with $\varepsilon = 0$. This figure identifies the important trend that in rocks with greater capillary retention, the plume remains more confined to the source and also that with a large drainage parameter, the current has a smaller run-out distance. The case with no capillary retention, $\beta = 1$, corresponds to the limit presented by Pritchard *et al.* (2001).

In the context of $CO_2$ sequestration, one of the key results from these calculations concerns the fraction of the original plume of $CO_2$ which remains trapped in the original layer, $V$. The variation of $V$ with $\Gamma$ and $\beta$ is shown in figure 3(*b*); if the pore-scale residual saturation of $CO_2$ has the value 0.3 ($\beta = 0.7$), and the permeable upper boundary has drainage parameter $0.01 < \Gamma < 1$, we find that only 0.4–0.6 of the injected $CO_2$ is trapped in the layer. With less pore-scale capillary trapping ($\beta > 0.9$), less than 20% of the $CO_2$ is retained in the layer as the plume spreads out and drains into the overlying layer.

For fixed $\Gamma$ the rate of draining also increases with $\varepsilon$ (for $\varepsilon \ll 1$), the dimensionless thickness of the thin seal layer.

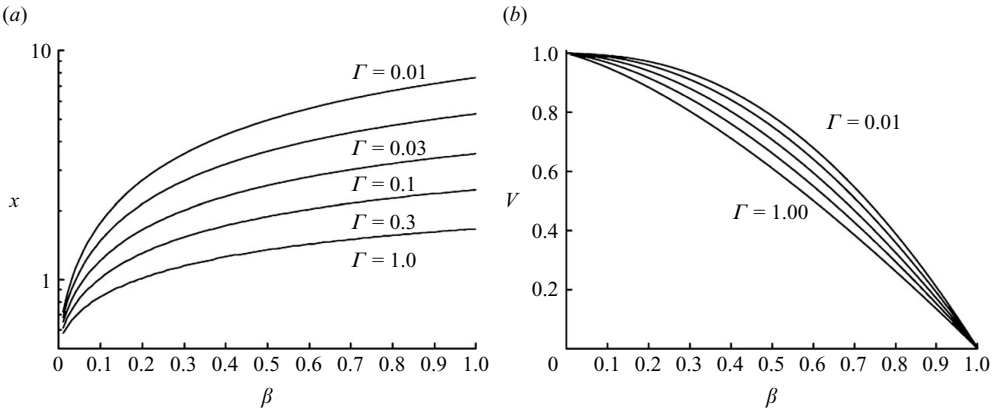


FIGURE 3. (*a*) Variation of the run-out distance of a current spreading on a horizontal surface, as a function of $\Gamma$ and $\beta$. (*b*) Variation of $V$, the fraction of the original $CO_2$ plume which is trapped in the formation through capillary retention, as a function of the draining parameter $\Gamma$ (0.01, 0.03, 0.1, 0.3, 1.0), and $\beta$.

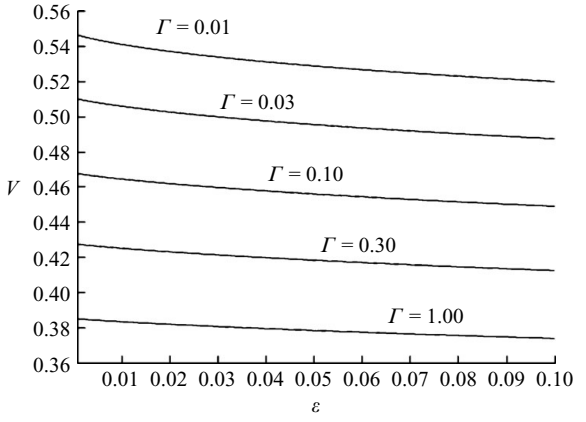


FIGURE 4. Effect of $\varepsilon$, the dimensionless thickness of the thin low-permeability layer on the fraction of the current which is trapped by capillary retention in the original flow layer. Curves are given for various values of $\Gamma$ with $\beta = 0.7$.

Indeed, in figure 4, we illustrate the variation of $V$ as a function of $\varepsilon$. The figure shows that the fraction which is retained decreases by 5%–10% as $\varepsilon$ increases from 0 to 0.1.

## 4. Sloping boundary

In many geological formations the strata are tilted, and this can have an important impact on the flow, in that there is a component of gravity which acts up as well as along the slope, leading to an asymmetry in the current shape as it evolves. To explore this we now present some solutions for the dispersal of the plume on a slope, starting with the same initial conditions as in § 3. The evolving shape of a typical plume on a slope is shown in figure 5.

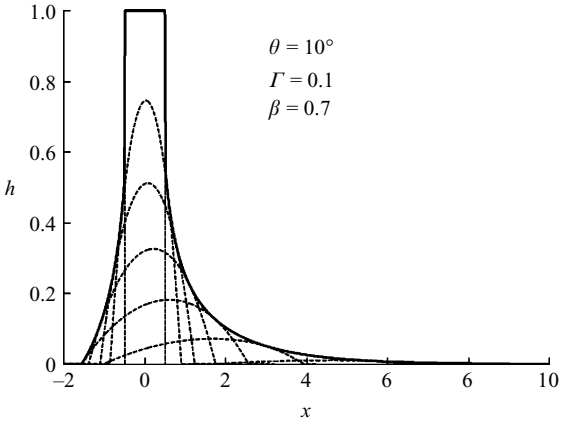


FIGURE 5. Variation of the shape of the current with time owing to the combination of draining through the boundary and capillary retention. Profiles are taken at times 0, 0.1, 0.33, 1.0, 2.5 and 7.5. In this calculation, the draining parameter $\Gamma = 0.1$, while a fraction 0.3 of the $CO_2$ within the pore spaces is assumed to remain trapped in the pores as the $CO_2$ plume is displacd by water ($\beta = 0.7$); for simplicity we set $\varepsilon = 0$. The initial shape is shown as the rectangular region $-0.5 < x < 0.5$, $h = 1$. The boundary of the region of rock which is contacted by the $CO_2$ plume is shown by the thick solid line, and it is in this region in which the $CO_2$ is trapped by capillary retention.

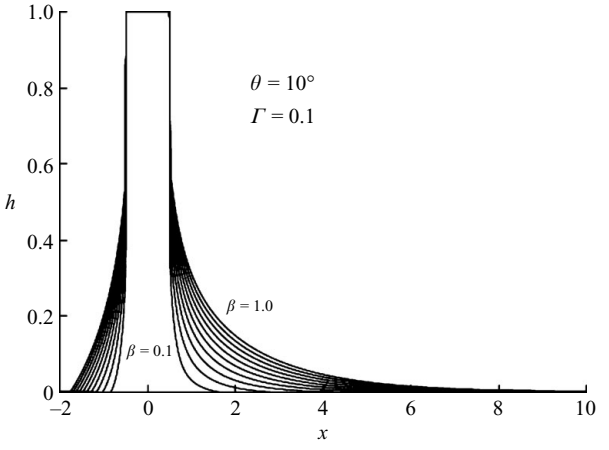


FIGURE 6. Variation of the locus of rock through which the plume passes as a function of the fraction of the current which is retained by the pores. Curves are shown in intervals of 0.1 for $\beta = 0.1$ to 1. In this figure $\Gamma = 0.1$, $\varepsilon = 0$ and $\theta = 10$.

As the plume spreads from the source it becomes progressively more elongated and asymmetrical, and the location of the maximum height in the plume becomes progressively located nearer the nose of the current, as a fraction of the overall length of the current. Also, the distance downslope of the source which is contacted by the fluid decreases.

The solid curve in figure 5 represents the locus of the region which is invaded by the plume and in which a cloud of residual fluid may become established. In figure 6 we illustrate how the zone of capillary-trapped fluid varies with $\beta$ for a fixed value of $\Gamma$, in the limit $\varepsilon = 0$. It is seen that as the fraction of the fluid which remains trapped

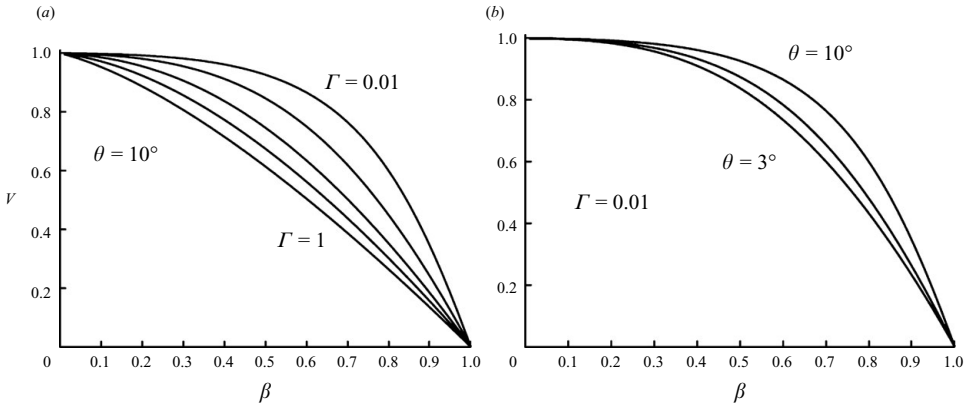


FIGURE 7. Variation of the fraction of the current which is retained in the original layer of rock as a function of $\beta$, the fraction of the pore space flooded by water at the trailing edge of the $CO_2$ plume. (*a*) Curves are shown for $\Gamma = 0.01$, 0.03, 0.1, 0.3 and 1 with $\theta = 10°$ and $\varepsilon = 0$. (*b*) Curves are given for angles 3°, 5° and 10° to the horizontal, in the case $\Gamma = 0.01$and $\varepsilon = 0$.

in the pore spaces increases ($\beta \to 0$), the region of rock through which the plume advances becomes smaller. This region represents the area in which $CO_2$ would be sequestered dynamically by capillary retention.

In order to illustrate the balance between the draining and the capillary retention, in figure 7(*a*), we show how $V$, the total fraction of the initial plume which is trapped in the pore spaces, varies with $\beta$. The remainder of the flow drains into the overlying layer. It is seen that the fraction of the plume which is trapped in the original flowing layer decreases rapidly as the pore-scale residual saturation of $CO_2$ decreases ($\beta \to 1$), and much of the fluid then drains into the overlying layers. Also, as with horizontally spreading currents (§ 3), as the residual saturation decreases, the current spreads laterally much further through the formation, leading to a larger area swept by the plume (figure 6).

The new parameter introduced in this section is the angle of slope, and this also has an important control on the fraction of the flow, which is retained in the original flowing layer compared to the fraction of the flow which drains. As the angle of slope increases, the along-slope flow speed increases, leading to a more rapidly receding trailing edge of the current and hence a greater amount of capillary retention compared to the draining. In turn this leads to a greater trapping of the fluid for the same values of the drainage parameter and capillary retention parameter. This effect is shown in figure 7(*b*). As for the case of a horizontal boundary (figure 4), we have found that as the dimensionless thickness of the thin seal layer, $\varepsilon$, increases from 0 to 0.1, the draining rate also increases for fixed $\Gamma$, and so there is a decrease in the fraction of the plume retained in the layer, although again for $\varepsilon < 0.1$ the reduction is less than about 10% of the overall volume of the plume (cf. Pritchard & Hogg 2002).

## 5. Aspect ratio

As well as the drainage parameter ($\Gamma$) and the capillary retention parameter ($\beta$) considered in the previous two sections, one of the other controls on the flow evolution is associated with the initial aspect ratio of the current. Let us consider a current with initial depth given by $h = 1/l_o$ for $-l_o/2 < x < l_o/2$ and $h = 0$ for $|x| > l_o/2$. In

the limit of a large initial aspect ratio $l_o^2$ (along-slope length/cross-slope thickness), the draining dominates the slumping of the flow, and the fraction of fluid which is retained in the pore space is close to the limit $1-\beta$, which would correspond to pure cross-layer draining, with no gravity-driven flow along slope. With deeper currents of smaller initial aspect ratio, more of the flow is retained as it spreads out laterally in the original flowing layer. To illustrate this effect, we can rescale the equations by introducing the parameters

$$h^* = \Gamma^{-1/3}h; \quad x^* = \Gamma^{1/3}x; \quad t^* = \Gamma t; \quad l_o^* = \Gamma^{1/3}l_o; \quad T = \Gamma^{-2/3}\tan\theta, \tag{8}$$

which leads to the equation

$$\left\{\begin{matrix}1\\ \beta\end{matrix}\right\}\frac{\partial h^*}{\partial t^*} = \frac{\partial}{\partial x^*}\left(h^*\frac{\partial h^*}{\partial x^*} - \mathrm{Th}^*\right) - h^* \quad \text{for} \quad \left\{\begin{matrix}\dfrac{\partial h^*}{\partial t^*} > 0\\ \dfrac{\partial h^*}{\partial t^*} < 0\end{matrix}\right\} \tag{9}$$

with initial conditions

$$h^* = \frac{1}{l_o^*} \quad \text{for } -\frac{l_o^*}{2} < x^* < \frac{l_o^*}{2} \quad \text{and} \quad h^* = 0 \quad \text{for } |x^*| > \frac{l_o^*}{2}. \tag{10}$$

It follows that the effect of increasing the initial aspect ratio ($l_o^2$) is similar to the effect of decreasing the drainage parameter ($\Gamma$), and therefore long, thin currents involve less capillary retention than shorter, deeper currents. Eventually, for very long thin currents, the flow primarily drains through the boundary, leaving only a fraction $(1-\beta)$ in the pore space.

## 6. Discussion

In assessing the effectiveness of $CO_2$ sequestration within a permeable rock, our simplified analysis has identified the important balance between the cross-layer draining through the boundary of a permeable layer and the capillary retention within that layer. These two parameters can provide insight into whether an injected plume of $CO_2$ would primarily be retained within the layer of rock in which it is injected, as a result of the lateral spreading, or whether the plume would tend to ascend through the boundary and spread both upwards through the layers and laterally. Field situations may involve a range of values of the capillary retention parameter (Barenblatt 1996; Hesse *et al.* 2006) and also the drainage parameter (Pritchard *et al.* 2001, Woods & Farcas 2008), so that in different situations, the drainage or the retention may dominate, leading to the different behaviours described herein.

As an example, suppose a volume of $10^6$ m$^3$ $CO_2$ was injected into a 1 km long well. With porosity 0.1, this would produce a plume spreading from the well with characteristic length scale 100 m. With low-permeability layers of thickness 0.1–1 m and permeability contrast $k/k_b \sim 10^3$, we expect $\Gamma \sim 0.1-1$. If capillary retention of gas in the pore spaces $(1-\beta) \sim 0.1$, then our calculations suggest that a fraction of the order 0.1–0.2 of the plume would be retained below a low-permeability horizon, and the remainder would drain upwards through the formation. Extrapolating from these results, we would then expect that after spreading through three or four layers, more than a half of the plume might be trapped within the formation.

The present analysis also points to some of the potential challenges of monitoring the fate of a plume of $CO_2$ in the subsurface following injection, owing to the multiple

flow paths which the $CO_2$ may follow, and the capillary retention of a small fraction of the plume throughout the region which is invaded by the $CO_2$, especially if on longer time scales this $CO_2$ dissolves into the unsaturated water. Various geophysical techniques are available for monitoring the injection of such a plume, including the processes of repeat seismic surveys, ground deformation and gravity studies. In the case of time lapse seismic monitoring, the reflection amplitude of seismic waves is measured at various times, and differences in these measurements are associated with changes in the pressure and fluid mixture (saturation) in the pore spaces of the rock. If there is some uncertainty associated with the capillary retention of fluid in the pore spaces, it can lead to uncertainty in the position of fluid fronts and the large-scale structure of the flow, and hence in the inversion of the data. Such quantitative uncertainties also lead to difficulties in accurate forward modelling of the subsurface dispersal of $CO_2$. By combining the output from the present model based on a simplified picture of the flow physics and the probability distributions for the uncertainties in the rock properties, risk-based analysis of the potential dispersal patterns of the $CO_2$ may be developed for hazard/risk assessment in selecting possible sites for sequestration.

## REFERENCES


Barenblatt, G. I. 1996 *Dimensional analysis, self-similarity and intermediate asymptotics.* Cambridge University Press.

Barenblatt, G. I., Entov, V. M. & Ryzhik V. M. 1990 *Theory of fluid flows through natural rocks.* Kluwer.

Bear, J. 1971 *Dynamics of flow in porous media.* Elsevier.

Bickle, M., Chadwick, A., Huppert, H. E., Hallworth, M., & Lyle, S. 2007 Modelling carbon dioxide accumulation at Sleipner: implications for underground carbon storage. *Earth Planet. Sci. Lett.* **255**, 164–176.

Mitchell, V. & Woods, A. W. 2006 Gravity driven flow in confined aquifers. *J. Fluid Mech.* **566**, 345–355.

Hesse, M. A., Tchelepi, H. A., Cantwell, B. J. & Orr, Jr., F. M. 2007 Gravity currents in horizontal porous layers: transition from early to late self-similarity. *J. Fluid Mech.* **577**, 363–383.

Hesse, M. A., Tchelepi, H. A. & Orr, Jr., F. M. 2006 Scaling analysis of the migration of $CO_2$ in aquifers: SPE 102796. In *2006 SPE Annu. Tech. Conf. Exhibition*, San Antonio, TX.

Hesse, M. A., Orr Jr., F. M. & Tchelepi, H. A. 2008 Gravity currents with residual trapping. *J. Fluid Mech.* **611**, 35–60.

Huppert, H. E. & Woods, A. W. 1995 Gravity-driven flows in porous layers. *J. Fluid Mech.* **292**, 55–69.

Kharaka, Y. K., Cole, D. R., Hovorka, S. D., Gunter, W. D., Knauss, K. G. & Freifeld, B. M. 2006 Gas water rock interactions in Frio Formation following $CO_2$ injection: implications for the storage of greenhouse gases in sedimentary basins. *Geology* **34** (7), 577–580.

Nordbotten, J. M. & Celia, M. A. 2006 Similarity solutions for fluid injection into confined aquifers. *J. Fluid Mech.* **561**, 307–327.

Obi, E.-O. I. & Blunt, M. J. 2006 Streamline-based simulation of carbon dioxide storage in a North Sea aquifer. *Water Resour. Res.* **42**, W03414, doi:10.1029/2004WR003347.

Press, W. H., Teukolsky, S. A., Vetterling, W. T. & Flannery, B. P. 1992 *Numerical recipes in Fortran 77.* Cambridge University Press.

Pritchard, D. 2007 Gravity currents over fractured substrates in a porous medium. *J. Fluid Mech.* **584**, 415–431.

Pritchard, D. & Hogg, A. J. 2002 Draining viscous gravity currents in a vertical fracture. *J. Fluid Mechanics* **459**, 207–216.

Pritchard, D., Woods, A. W. & Hogg, A. J. 2001 On the slow draining of a gravity current moving through a layered permeable medium. *J. Fluid Mech.* **444**, 23–47.

Qi, R., Beraldo, V., LaForce, T. & Blunt, M. J. 2007 Design of carbon dioxide storage in the North Sea using streamline-based simulation: SPE 109905. In *SPE Annu. Tech. Conf. Exhibition*, Anaheim, CA.

Riaz, A., Hesse, M. A., Tchelepi, H. A. & Orr, F. M. 2007 Onset of convection in a gravitationally unstable diffusive boundary layer in porous media, *J. Fluid Mech.* **548**, 87–111.

Woods, A. W. 1998 Vaporizing gravity currents in superheated porous rock. *J. Fluid Mech.* **377**, 151–168.

Woods, A. W. & Farcas, A. 2009 On the leakage of gravity currents advancing through sloping layered permeable rock. *J. Fluid Mech.* **618**, 361–379.